Smart Structures and Systems, *Vol. 30, No. 4 (2022) 411-420*
https://doi.org/10.12989/sss.2022.30.4.411

Identification of structural displacements utilizing concurrent robotic total station and GNSS measurements

Hüseyin Pehlivan*

Department of Geomatics Engineering, Faculty of Engineering, Gebze Technical University, Kocaeli, Turkiye

(*Received November 29, 2021, Revised May 2, 2022, Accepted July 4, 2022*)

Abstract. Monitoring large structures is a significant issue involving public health on which new studies are constantly carried out. Although the Global Navigation Satellite System (GNSS) is the most preferable method for measuring structural displacements, total stations, one of the classical geodetic instruments, are the first devices that come to mind in cases that require complementary usage and auxiliary measurement methods. In this study, the relative displacements of the structural movements of a tower were determined using robotic total stations (RTS) and GNSS. Two GNSS receivers and two RTS observations were carried out simultaneously for 10 hours under normal weather conditions. The spectral analysis of the GNSS data was performed using fast Fourier transform (FFT), and while the dominant modal frequencies were determined, the total station data were balanced with the least-squares technique, and the position and position errors were calculated for each measurement epoch. It has been observed that low-frequency structural movements can be determined by both methods. This result shows that total station measurements are a helpful alternative method for monitoring large structures in situations where measurements are not possible due to the basic handicaps of GNSS or where it is necessary to determine displacements with short observations.

Keywords: FFT; GNSS; robotic total station; structural displacement; the least-squares method

1. Introduction

Depending on the developments in building design and construction, each of gigantic structures continues to develop more comprehensively and more functionally than the previous one. Structural monitoring studies are also progressing with new studies and experiments to protect structural health and public safety, extend the service life of buildings and take precautions against disasters. The primary purpose of these monitoring systems is to determine the position changes and actual displacement magnitudes of the structural responses as a function of time by monitoring them continuously or periodically. Measuring oscillations and vibrations that affect structural health with the most appropriate measurement techniques and calculating the modal parameters of these movements with correct data analysis techniques are the major research subjects. Two important parameters in the selection of the most suitable measuring sensors in structural monitoring are the accuracy and cost of the measurement. Recent studies on SHM have generally focused on obtaining more easygoing observation measurements and lower costs without sacrificing the expected accuracy (Jo *et al*. 2013, Zhao *et al*. 2015).

Many studies have been conducted using different measurement methods to collect observation data in structural health monitoring (SHM) works of structures of various types, sizes, and geometries (Psimoulis and Stiros 2007, 2013, Psimoulis *et al*. 2008, Moschas and Stiros 2011, Chatzi and Fuggini 2012, Kaloop *et al*. 2016, Casciati and Vece 2017, Shen *et al*. 2019, Stiros *et al*. 2019, Yu *et al*. 2020). In general, the measurement methods to be used in SHM work and the selection of measurement sensors depend on the expected accuracy in modeling the predicted static and dynamic movements of the structure. This expected accuracy requirement is also related to the purpose of the measurements, the magnitude, and the direction of the expected deformation and displacement movements. The accuracy expectation is also directly related to the sampling interval or sampling frequency of the measuring instruments we use. Namely, according to the Nyquist theorem, we need to measure with a sampling frequency of twice the magnitude of the structural natural frequency we want to determine (Pehlivan and Bayata 2016, Wang *et al*. 2021). Accordingly, if the structural vibration frequency is in the range of 0–10 Hz, the sampling frequency of the measuring sensor should be 20 Hz or higher.

When we consider measuring instruments in this context, non-destructive sensors such as accelerometers, inclinometers, strain gauges, and anemoscopes are often used to determine vibration modes. However, although these sensors are sufficient for monitoring vibration frequencies, they are insufficient to detect long-term quasi-static displacement changes (Wang *et al*. 2021). In general, geodetic measurement methods are preferable when it comes to determining the structural displacement sizes. We can record 3D coordinates as a function of time during the construction and operation of structures by using the most

*Corresponding author, Ph.D., Assistant Professor,
E-mail: hpehlivan@gtu.edu.tr

ISSN: 1738-1584 (Print), 1738-1991 (Online)

preferred Global Navigation Satellite System (GNSS). Numerous studies have been conducted in which GNSS has been used alone or in combination with different structural monitoring studies (Kaloop *et al*. 2016, Roberts *et al*. 2004, Lekidis *et al*. 2005, Chan *et al*. 2006, Meng *et al*. 2007, Breuer *et al*. 2015, 2021, Yigit *et al*. 2016, Moschas and Stiros 2011, Psimoulis and Stiros 2013, Pehlivan *et al*. 2015, Yu *et al*. 2016, Wang *et al*. 2021). Apart from this, as geodetic measurement methods, Robotic Total Station (RTS) (Psimoulis and Stiros 2007, Erdoğan and Gülal 2013), ground photogrammetric equipment (Yu *et al*. 2016, Erdoğan and Gülal 2013), 3D laser scanners (Kaloop and Li 2009), Ground-based Synthetic Aperture Radar (GB-SAR) (Lienhart *et al*. 2017, Zhou *et al*. 2020), GNSS (Kaloop *et al*. 2015, Moschas *et al*. 2013), many structural monitoring methods have been used (Shen *et al*. 2019, Wang *et al*. 2021, Park *et al*. 2007).

The primary measurement tool that provides accuracy and economic criteria in structural monitoring is GNSS technology, and it can model structural movements in all weather conditions. In recent years, GNSS receivers with a sampling rate of 10-100 Hz have been produced and used in structural dynamic monitoring with higher accuracy (Kaloop and Li 2009, Kaloop *et al*. 2015, Yu *et al*. 2014, Moschas and Stiros 2011, Xu *et al*. 2002). In addition, the continuous development of software and hardware and the high sampling interval have provided significant advantages in monitoring their structures. With this method, it is possible to determine the dynamic and static displacements of the structure or the resulting deformations in real-time. However, there are cases where the GNSS method is also insufficient. The most important limitation is that uninterrupted satellite visibility is required to achieve successful results in GNSS measurements. In such cases, noisy data will be obtained where multipath will be very effective (Pehlivan and Bayata 2016).

Research shows that GNSS systems cannot be used, especially in structures where installation costs are high, and multipath may be excessive. In addition, although successfully used in high-rise buildings, bridges, and dams, GNSS receivers installed on the side faces of tower structures, which block and reflect satellite signals by tower walls, make it impossible to detect small-amplitude oscillations. Although an alternative measurement sensor to GNSS has not yet been developed, some other tools integrated with GNSS are used to determine static and dynamic movements. In these cases, the use of the total station, which is a traditional measurement method, has come to the fore as an alternative measurement method. Important geodetic devices such as robotic total stations or automated theodolites are one of them and are used as auxiliary and alternative tools to GNSS (Psimoulis and Stiros 2007, 2008, 2011, 2013, Stiros *et al*. 2019, Zhou *et al*. 2021). Numerous studies have been conducted using RTSs in combination with other measurement tools.

The total stations allow us to monitor the movement of observation points (towers, buildings, bridges, and dams) with the ability to periodically record angle, distance, and time measurements. In recent years, better results have been obtained in SHM studies with its automated structure, increased sampling frequencies, and robotic features. It is possible to determine movements in the 2-10 Hz range by using RTSs that can be self-directed to the target with the servo motor feature. Because of these advantages, it is widely used in many structural monitoring and other engineering projects (Psimoulis and Stiros 2008, Moschas *et al*. 2013, Lienhart *et al*. 2017, Stiros *et al*. 2019).

Many scholars have been interested in using RTS in structural monitoring studies. Psimoulis and Stiros (2008, 2011, 2013) performed important studies using RTS to determine the displacement of railway bridges and pedestrian bridges. Robotic theodolites have been used to determine the displacements of short-span bridges with millimeter precision (Psimoulis and Stiros 2011). When trains crossed a railway bridge, Psimoulis *et al*. (2008) measured deviations of 2.5–6 mm, and vibrations of up to 1.3 mm when they did not. The accuracy limits that can be obtained in RTS-based deformation monitoring have been studied in recent years (Frukacz *et al*. 2017). The accuracy limits in RTS-based structural monitoring that can be attained are still being researched and interest researchers' attention (Frukacz *et al*. 2017). The results of using modern geodetic sensors to determine a structure's dynamic response are presented (Kovai and Motoh 2019). Stiros *et al*. (2019) examined the response of different bridge types to traffic loads using measurement techniques such as RTS, GNSS, and accelerometers. Another study shows the methods for selecting and evaluating a monitoring station's position accuracy, as well as the results of using the least squares method (Hatoum and Mustafin 2020).

This article presents a case study using an automated total station and RTK GNSS simultaneously to determine the relative displacements of a 220 m high tower. Measurements were made with two GNSS receivers and two RTS, in contrast to previous studies, in order to provide full comparative control of the measuring instruments (Fig. 1). For GNSS data, the spectral analysis method with the Fourier transform was used to determine significant frequency values, and the least squares method was used to determine statistical significance estimates and compare accuracies in RTS data. RTS observations were made at an average distance of 550 m from the reflectors, which were positioned at a height of 165 m from the tower. Measured and recorded angle-distance observations were balanced with the least-squares method in each measurement period, and the coordinates and position errors of the tracking points were calculated. According to the results obtained with both measurement methods, it was observed that the slow movements were consistent in determining the displacement changes. That is, long-term (low frequency) displacements obtained from RTS with a sampling period of about 2 minutes and displacements obtained from GNSS data with a sampling period of 20 Hz were found to be consistent. However, it has been observed that GNSS data is more efficient in detecting short-term (high-frequency) displacements.

2. Materials and methods

The test measurements were carried out in a tower where structural movements have a slow character. Under

normal weather conditions, the structure will make a slow oscillation with the effect of dominant loads such as temperature and wind. For these reasons, it is thought that performing our observations with a sampling interval of a few minutes of RTS measurements will allow us to determine the expected movements in monitoring the expected constant and regular motion under normal atmospheric conditions.

Today, modern RTSs can accurately measure the angle value in the range of 0.5-1cc and the length in the range of 0.6-1 mm per 1 km (Psimoulis and Stiros 2007, Trimble 2021, Zhou *et al*. 2020). Distance and angle measurements give noisy results with the effect of the servo motor mechanism (Radovanovic and Teskey 2001, Cosser *et al*. 2003). However, the calculation of coordinates by the least-squares method of angle and length measurements at long distances can provide relief from this long-term noise (Psimoulis and Stiros 2007). On the other hand, due to the law of propagation of errors (Alsadik 2019), Cartesian coordinates calculated from polar coordinates tend to be characterized by higher accuracy (or precision), usually with an accuracy of 1-2 mm (Trimble 2021, Cook 2006).

In structural monitoring measurements, it is possible to determine the coordinates with an accuracy of 1-2 mm with the RTS, and the precision of each measured displacement can also be determined (Psimoulis and Stiros 2007, Alsadik 2019). Due to the nature of RTS measurements, repeated angle-distance measurements under the same conditions and the Cartesian coordinates derived from them provide high precision, and noise will be limited in a prominent region while measurement accuracy will increase.

2.1 Workspace and experimental test data

It is predicted that the tower will have long-term and short-term behaviors in its motion spectrum. We aim to determine the displacement magnitudes of the most dominant, low, and high-frequency movements during the measurement period as a function of time. For this purpose, test data were obtained with the measurement system presented in Fig. 1. To provide complementary and control measurements, GNSS receiver antennas and total station prisms were placed at the same observation points at 165 m height, in the same vertical direction (Fig. 1). In this way, it was aimed at making simultaneous observations at the same observation points with GNSS and RTS.

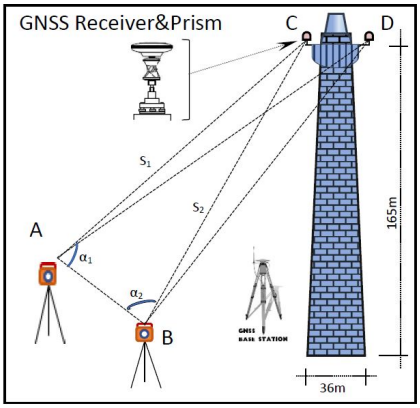

Fig. 1 The layout of test measurement system

Observations were recorded at sampling intervals of 0.05 seconds with GNSS and approximately 2 minutes with RTS. In this case, while lower frequency movements can be determined with GNSS data, it is expected that the same periodic movements of 2 minutes or more can be determined by both measurements. For this purpose, according to the measurement system shown in Fig. 1, observations were made from the total stations installed at points A and B to prisms mounted at points C and D, and simultaneous measurements were also carried out with GNSS receivers.

2.2 Determining adjusted coordinates with the least squares method

The main focus of this research is to test can be the use of RTSs as well as GNSS in determining structural movements. Therefore, the methodology followed for detailed examination and analysis of RTS data is presented in this section. Four observations, two distances and two angular directions, were made to each of the C and D observation points with the automatic total station devices installed at two fixed station points, such as A and B with RTS. Observations were carried out simultaneously between 11 a.m. and 5 p.m. The observations at points C and D were evaluated separately, but with the same mathematical model. Only the mathematical model for observation point C is presented here.

With an angular-linear intersection for the observation point C or D, the number of observations is greater than the unknown, so the least-squares method can be used to determine their coordinates. The linear-angular intersection method was used to determine the accuracy of the coordinates of the observation point to be determined by the angle-distance measurements made with the total station and to take advantage of the least-squares method (Okwuashi and Asuquo 2012, Ehigiator and Ehigiator–Irughe 2018, Ehigiator-Irughe *et al*. 2010, Ehigiator *et al*. 2017).

Observations were made to prism point C with two total stations installed and leveled at A and B points. Horizontal and vertical angle values and oblique length values were recorded at equal time intervals for six hours. Vertical angles, oblique length measurements, and horizontal distances S_1 and S_2 were calculated. Horizontal angles α_1 and α_2 and horizontal distances S_1 and S_2 measurements were obtained as time series for each measurement interval. Using these data, the coordinates of the prism point (C) were determined by observations made from A and B. The balancing of the calculated coordinates will be done using the observation equation method. The coordinates of the observed prism point are (Xc, Yc); the coordinates of the fixed station points A and B are (XA, YA) and (XB, YB), respectively.

The adjustment in this case is carried out using the method of the observation equation. It is assumed that the weight of all measurements made is the same (W = I). In this adjustment model (observational least square), the number of equations is equal to the number of observations (n = 4). Each equation contains one observation and one or

more unknowns. In this case, observations are (S_1, S_2, α_1, α_2) and unknowns are (Xc, Yc). The two lengths (S_1, S_2) of the lines in the horizontal projection can be written in a coordinate form as follows

$$\begin{aligned} S_1 &= \sqrt{(X_C - X_A)^2 + (Y_C - Y_A)^2} \\ S_2 &= \sqrt{(X_C - X_B)^2 + (Y_C - Y_B)^2} \end{aligned} \tag{1}$$

The horizontal angles (α_1 and α_2) from Fig. 1 can be calculated as follows

$$\begin{aligned} \alpha_1 &= cos^{-1}\left(\frac{\overline{AC}^2 + \overline{AB}^2 - \overline{CB}^2}{2\,\overline{AC}\,\overline{AB}}\right) \\ \alpha_2 &= cos^{-1}\left(\frac{\overline{BA}^2 + \overline{BC}^2 - \overline{AC}^2}{2\,\overline{BA}\,\overline{BC}}\right) \end{aligned} \tag{2}$$

Using the coordinates of the points, we can write equations 2 as follows

$$\begin{aligned} \alpha_1 &= cos^{-1}\left[\frac{(X_C - X_A)^2 + (Y_C - Y_A)^2 + AB^2 - (X_C - X_B)^2 + (Y_C - Y_B)^2}{2\,AB\,\sqrt{(X_C - X_A)^2 + (Y_C - Y_A)^2}}\right] \\ \alpha_2 &= cos^{-1}\left[\frac{(X_C - X_B)^2 + (Y_C - Y_B)^2 + \overline{AB}^2 - (X_C - X_A)^2 + (Y_C - Y_A)^2}{2\,\overline{AB}\,\sqrt{(X_C - X_B)^2 + (Y_C - Y_B)^2}}\right] \end{aligned} \tag{3}$$

The four observation equations given in Eqs. (1)-(3) are nonlinear functions of both parameters and observations; they can be worked out using the least-squares adjustment technique. Before you start solving, approximate values of unknown parameters are calculated. The approximate values of the coordinates of the C point are calculated using the angular intersection according to the following formulas (Ehigiator and Ehigiator–Irughe 2018, Ehigiator-Irughe *et al*. 2010, Ehigiator *et al*. 2017, Pehlivan 2021)

$$\begin{aligned} X_C^0 &= \frac{X_A\,cot\,\alpha_2 + X_B\,cot\,\alpha_1 - Y_A + Y_B}{cot\,\alpha_1 + cot\,\alpha_2} \\ Y_C^0 &= \frac{Y_A\,cot\,\alpha_2 + Y_B\,cot\,\alpha_1 - X_A + X_B}{cot\,\alpha_1 + cot\,\alpha_2} \end{aligned} \tag{4}$$

Using these X_C and Y_C values, the approximate values of the observation equations (L_o) are calculated. Then the misclosure vector (L) is calculated as

$$L = L^0 - L_{abs} \tag{5}$$

We can express the linearized model in matrix form as follows

$$V_{4\times1} = A_{4\times2}\,.X_{2\times1} + L_{4\times1} \tag{6}$$

Where; A: The coefficients matrix of parameters, L: The misclosure vector, V: The residuals vector. Matrix A may be computed by differentiation of the four equations concerning the two unknowns and can be written in the form

$$A_{(4\times2)} = \begin{bmatrix} \frac{\partial S_1}{\partial X_C} & \frac{\partial S_1}{\partial Y_C} \\ \frac{\partial S_2}{\partial X_C} & \frac{\partial S_2}{\partial Y_C} \\ \frac{\partial \alpha_1}{\partial X_C} & \frac{\partial \alpha_1}{\partial Y_C} \\ \frac{\partial \alpha_2}{\partial X_C} & \frac{\partial \alpha_2}{\partial Y_C} \end{bmatrix} \tag{7}$$

The elements of the matrix A (a_{ij}) can be obtained using the Matlab software by differentiating the four observation equations. And thus the normal equation system is written as follows

$$N_{2\times2}.\hat{X}_{2\times1} + U_{2\times1} = 0 \tag{8}$$

Where

$$N_{2\times2} = A^T_{2\times4}.W_{4\times4}.A_{4\times2} \tag{9}$$

And

$$U_{2\times1} = A^T_{2\times4}\,.W_{4\times4}\,.L_{4\times1} \tag{10}$$

The solution for the normal equation system (8) is as follows

$$\hat{X}_{2\times1} = -N^{-1}_{2\times2}.U_{2\times1} \tag{11}$$

Following that, the unknown parameters that have been adjusted can be calculated as follows

$$\bar{X}_{2\times1} = \hat{X}_{2\times1} + X^0_{2\times1} \tag{12}$$

The vector of adjusted observations can be estimated as follow

$$\bar{L}_{4\times1} = \hat{V}_{4\times1} + L_{4\times1} \tag{13}$$

The variance factor that has been estimated is

$$\sigma_0^2 = \frac{V^T.W.V}{r} = \frac{V^T.W.V}{2} \tag{14}$$

The estimated variance-covariance matrix of the parameters is as follows

$$C_X = \sigma_0^2\,.N^{-1} \tag{15}$$

And as a result, the variance-covariance matrix of adjusted observations is computed follow as

$$C_L = A\,.\,C_X\,.A^T \tag{16}$$

This normal Eq. (16) with using the Matlab program can be solved. The positional error at point C can be computed

using the following equation (Allan 1988)

$$M_C = \frac{b\, m_\alpha^{"}}{\rho^{"} \sin\gamma} \sqrt{sin^2_{\alpha_1} + sin^2_{\alpha_2}} \quad (17)$$

Where; b: Base line (the distance between total stations) (b = AB in Fig. 1); $m_\alpha{}^{cc}$: Mean square error of measuring horizontal angles (taken from specifications of the using total stations); ρ"=206265", γ: The horizontal angle at point C. To accept the observations of point C from the triangle ABC and its adjusted coordinates to be sufficiently accurate, the coordinates must satisfy the following criterion (Ehigiator-Irughe *et al*. 2010, Pehlivan 2021).

$$r_C = \sqrt{\Delta_x^2 + \Delta_y^2} \leq M_t \quad (18)$$

Where;

$\Delta_X = X_i^C - X_i^0$, $\Delta_Y = Y_I^C - Y_I^0$ and $M_t = \sqrt{M_1^2 + M_2^2}$, X_i^0, Y_I^0: The raw coordinates of the point C at the time i of measurement; X_I^C, Y_I^C: The adjusted coordinates of the point C at the time i of the measurement; M_1 and M_2: The position errors of the point C at the time I (Ehigiator-Irughe *et al*. 2010, Pehlivan 2021).

2.3 Determining the structural displacements

We utilize the coordinates XiYi and XkYk at i and k times, respectively, to determine a 2-dimensional displacement of an observation point.

The displacement in the time interval Δt will be $dn = \sqrt{\Delta x^2 + \Delta y^2}$.

Where; $\Delta t = t_k - t_i$; time difference between two periodic measurements. $\Delta x = x_k - x_i$, the x-axis displacement $\Delta y = y_k - y_i$, the y-axis.

Δx and Δy each represent a motion vector when expressed as coordinate differences of point displacements. And each has a magnitude and direction. The sum of the absolute values of these point displacements gives the total displacement during the measurement period. The following formula is used to determine if the displacement at time dt remains within the error limits, taking into account the measurement errors at I and k points

$$|dn| < (pn) \quad (19)$$

Where; dn is the magnitude of the displacement (for point n), (pn) = maximum magnitude of the combined 95% confidence ellipse for point n = (1.96).

$pn = \sqrt{\sigma f^2 + \sigma i^2}$ and σf is the standard error of the following position measured, and σi is the standard error of the first measured position.

3. Analysis of RTS test data

As shown in Fig. 1, From the fixed station points (A and B), observations were made to the C and D observation points every 2 minutes and the data sets (2 edges and 2 angle values) were recorded as a function of time. The observations (angles and lengths) from station points A and B to point C are presented in Fig. 2. Similarly, the observations (angles and distances) from station points A and B to point D are presented in Fig. 3.

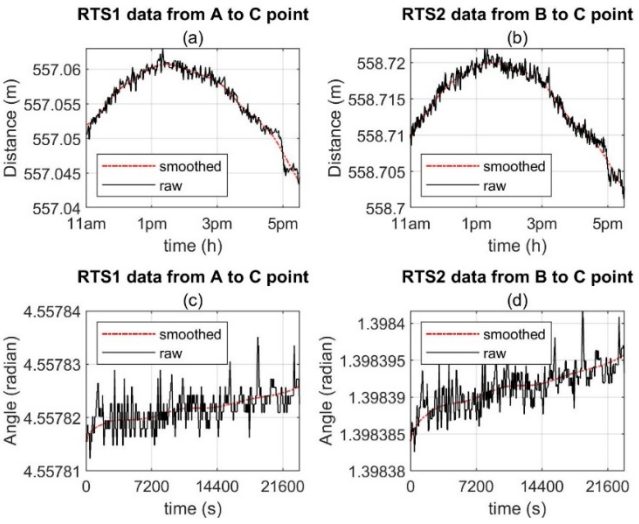

Fig. 2 Time series diagram of the original observation data.
(a) Length observations from point A to point C;
(b) Length observations from point B to point C;
(c) Angle observations from point A to point C;
(d) Angle observations from point B to point C

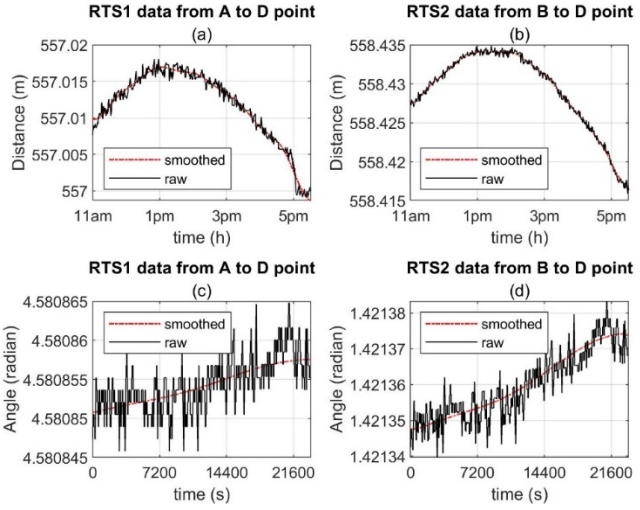

Fig. 3 Time series diagram of the original observation data.
(a) Length observations from point A to point D;
(b) Length observations from point B to point D;
(c) Angle observations from point A to point D;
(d) Angle observations from point B to point D

Each observation data set was pre-checked in itself, with the goal of establishing 5-minute observation sets to measure the change in overall displacement over time. For this purpose, the balanced coordinate values (XC, YC and XD, YD) of observation points C and D every 5 minutes between 11:00 and 17:00 were calculated in MATLAB using the least-squares equation model (as given in section2.2). Also, position errors (M_C and M_D) at points C and D were calculated for each adjustment time using Eq.

Table 1 Accuracy test of adjusted coordinates of observed points C and D

Time	C Point			D Point		
	Δx (mm)	Δy (mm)	$r_C\ (\leq M_t)$ (mm)	Δx (mm)	Δy (mm)	$r_D\ (\leq M_t)$ (mm)
11:30	0.13	0.57	0.59	0.006	-1.09	1.09
12:00	0.05	0.30	0.309	-0.013	-1.07	1.07
12:30	-0.06	-0.02	0.06	-0.012	-0.47	0.472
13:00	-0.13	-0.19	0.23	-0.033	-0.86	0.859
13.30	-0.11	-0.21	0.24	-0.011	-0.436	0.436
14:00	0.02	-0.07	0.07	0.0001	-0.144	0.144
14:30	0.20	0.41	0.46	0.0370	0.38	0.383
15:00	0.10	0.24	0.27	0.0274	0.720	0.722
15:30	-0.06	-0.24	0.25	0.0400	1.065	1.066
16:00	-0.26	-0.71	0.75	-0.0100	0.392	0.392
16:30	0.04	-0.08	0.09	-0.0014	0.644	0.644
17:00	0.07	-0.01	0.07	-0.0296	0.871	0.872

Table 2 The displacement changes of the observed points

Time	C Point			D Point		
	Δx (mm)	Δy (mm)	$\mathrm{dn} = \sqrt{\Delta x^2 + \Delta y^2}$	Δx (mm)	Δy (mm)	$\mathrm{dn} = \sqrt{\Delta x^2 + \Delta y^2}$
12:00	0.08	-1.41	1.41	0.14	-1.95	1.96
12:30	0.33	-2.53	2.55	0.48	-3.64	3.67
13:00	0.47	-1.98	2.04	0.59	-2.99	3.05
13.30	0.79	-1.38	1.59	0.87	-2.37	2.53
14:00	1.09	-0.23	1.11	1.19	-1.04	1.58
14:30	1.50	1.02	1.82	1.53	0.42	1.58
15:00	1.83	2.15	2.82	1.81	1.77	2.54
15:30	2.10	3.09	3.73	2.06	2.91	3.57
16:00	2.09	3.29	3.90	1.96	3.29	3.83
16:30	2.28	3.71	4.35	2.10	3.80	4.34
17:00	1.09	1.80	2.10	0.97	1.91	2.14

(17). Because each set of balanced measurements is affected by approximately the same parameters, positional error values with very minor deviations (3,825 mm) were obtained for each set of balanced measurements.

Eq. (18) was used to test the accuracy of the adjusted coordinate values of the points C and D. Mt values were calculated for each measurement period using the calculated position errors (Mt = 5.41). As a result of the comparison of rp and Mt values, it was acceptable that the observations made to point C in triangle ABC and its corrected coordinates are sufficiently accurate. Corrected coordinates and accuracy test results calculated from 5-minute sample sets of data recorded during the observation period are presented in Table 1 for each 30-minute mean value.

Similarly, the rp and Mt values were given in equation 18 (Mt = 5.41) were also calculated for point D. It was accepted that the observations made to point D in triangle ABD, as well as its adjusted coordinates, were accurate adequate.

The displacements at the C and D points during the measurement span were calculated from the adjusted and smoothed coordinates in the X and Y axis. The displacement amplitudes (dn) and standard errors of displacement (pn = 5.41) were computed at each periodic n point and compared using Eq. (19). Table 2 shows that the computed displacements amplitudes are less than the error limit.

The magnitude of the displacement (dn) at each periodic n point was calculated and the measurement accuracy of the displacements [|dn| < (pn = 5.41)] (Eq. (19)) values were calculated from the formula (Table 2). As a result, the displacements calculated for each equilibration time remained within the 95% confidence ellipse.

4. Analysis of GNSS data

GNSS observations were also taken during the test measurement with a sampling interval of 0.05 seconds, and the X, Y, and Z coordinates of the C and D observation points were recorded as a function of time. Because there is no expected vertical movement at the observation points,

Table 3 The highest amplitude dominant frequency values of the GNSS data at point C

Freq. No	Freq. (Hz)	Period (sec.)	Amp. (m)	Phases (Deg.)	Angular Freq. (Hz)
f1	0.00001157	86400.00	0.0482	-179.96455	0.00007272
f2	0.00013889	7200.00	0.0020	144.75748	0.00087266
f3	0.00038194	2618.18	0.0017	55.39479	0.00239983

*f1: Calculated Frequency for 1st mode; f2: Calculated Frequency for 2nd mode; f2: Calculated Frequency for 3rd mode

Table 4 The highest amplitude dominant frequency values of the GNSS data at point D

Freq. No	Freq. (Hz)	Period (sec.)	Amp. (m)	Phases (Deg.)	Angular Freq. (Hz)
f1	0.00001157	86400.00	0.0370	-179.53211	0.00007272
f2	0.00010417	9600.00	0.0010	-169.30866	0.00065450
f3	0.00018519	5400.00	0.0009	-121.37421	0.00116355

*f1: Calculated Frequency for 1st mode; f2: Calculated Frequency for 2nd mode; f2: Calculated Frequency for 3rd mode

Table 5 Re-constructed signals with selected frequencies

Reconstructed Signal	Sampling Rate (Sec.)	Selected Frequencies	Standard Deviation (m)
1st mode	1	f1	0.00815
2nd mode	1	f1, f2	0.00527
3rd mode	1	f1, f2, f3	0.00474

the structural displacement changes are calculated as 2D in the X and Y axes. The spectrum analysis method was used to determine the displacement changes in the X and Y series. Firstly, the 24-hour long X/Y series (GNSS data) were resampled with a 1-second sampling interval and filtered in the time domain, taking into consideration the measurement time and sampling frequency. The FFT (Fast Fourier Transformation) transform was used to separate it into sub-signals, and all sub-frequency values and amplitude values corresponding to these signals were calculated. When we sorted the lower frequency values from greatest to smallest depending on their amplitude values, we saw that the first three frequency values stood out. Tables 3 and 4 show the dominant f1, f2, and f3 frequency values in the X/Y series at observation positions C and D, as well as the amplitude, period, phase, and angular frequency values.

The frequency values presented in Tables 3 and 4 are considered to be modes expressing the dominant displacement movements seen at points C and D. It has been evaluated that the f1 frequency value modeled a 24-hour movement, the f2 frequency modeled a repetitive oscillation with a period of 2 hours and 40 minutes, and the f3 frequency modeled an oscillating movement of 1.5 minutes. Using these first three frequency values that were found to be significant, each X/Y signal was reconstructed by the IFFT (Inverse Fast Fourier Transformation) process. The standard deviations of the series created with three different modes of these filtered and clean displacement movements are given in Table 5.

In the displacement changes modeled using the three mode values given in Table 5, it was evaluated that the 1st mode represents the dominant displacement movement during the measurement period (i.e., one day). The other 2nd and 3rd modes are oscillatory modes that take place in shorter periods. The spatial displacement changes of observation point C are modeled using three dominant

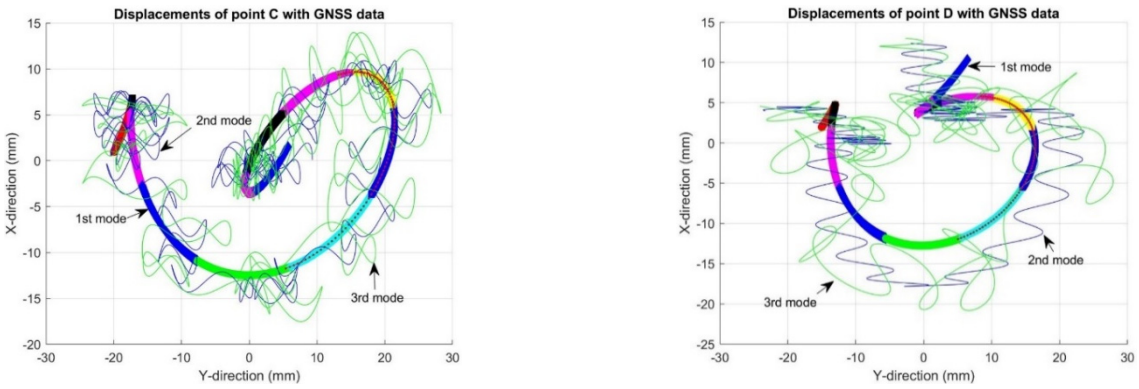

(a) C observation point (b) D observation point

Fig. 4 Positional displacements plotted with GNSS data

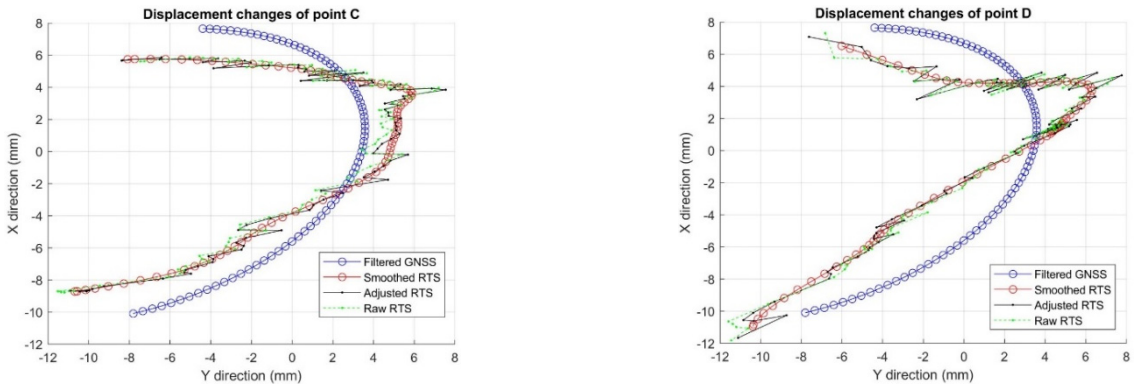

(a) C observation point (b) D observation point

Fig. 5 Positional displacements plotted with RTS and GNSS data

modes of GNSS data, as shown in Fig. 4(a). The 1st mode position changes were colored differently in each of the two-hour time zones.

5. Accuracy evaluation of displacement quantities with GNSS and RTS measurements

The displacement changes of the C and D points, which were observed simultaneously with RTS and GNSS between 11:00 and 17:00, were compared and evaluated. Accordingly, at observation point C. The magnitude of the total displacement from the balanced RTS coordinates was calculated as 27.433 mm. According to these calculations, it was determined that the structural displacement was approximately 2.7 cm from the six-hour measurements made with RTS. Fig. 5(a), shows the spatial displacements of the observation point C plotted with raw and corrected coordinates in the X/Y plane to time. When the normalized 6-hour GNSS data is also overlay, the data shown that they are consistent.

At observation point D: The magnitude of the total displacement from the balanced RTS coordinates was calculated as 30,779 mm. According to these calculated results, it was determined that the structural displacement was approximately 3.0 cm from the six-hour measurements made with RTS. Fig. 5(b) shows the spatial displacements of observation point D plotted based on time using raw and corrected coordinates in the X/Y plane. The displacement changes appear to be consistent when the normalized 6-hour GNSS data is also overlaid.

The analysis of the RTS data with the least-squares method has given the result that the obtained results are reliable. Figs. 5(a) and 5(b) show that most of errors in RTS data are within ± 2 mm and that extreme deviations are very rare. The same figures show displacements calculated by superimposing RTS and GNSS measurements using data processing methods. These results show that the RTS data provides the computational results closest to the actual displacements. According to these results, the static displacements computed from RTS and GNSS data are quite similar.

6. Conclusions

Previous researches that used GNSS and RTS together compared these two different measuring techniques, which differ in terms of measurement technique, technology, and error sources, and showed their usability in monitoring bridges and structures. To determine structural displacements, GNSS and RTS measurements were collected and processed simultaneously in this study. However, unlike prior studies, a new methodology was employed in the analysis of simultaneous GNSS and RTS data. While the GNSS data were analyzed spectrally in terms of time and frequency, the least squares adjustment method was used to determine the accuracy of the RTS data, and thus the displacement changes corresponding to the tower's horizontal movement were determined. The collected data by both techniques was assessed in terms of reliability and sampling frequency, and a more meaningful comparison of the two methods could be made.

In this experiment, RTS, which can measure with a period of about 2 minutes, and GNSS, which records measurements with a period of 0.05 seconds, was used, and the mean horizontal displacement of 3.0 cm and 3.8 cm, respectively, were determined from the RTS and GNSS data. While oscillations of 5-10 mm amplitude and structural movements with a period of about 2 minutes can be determined with GNSS, oscillations of a few mm amplitude and longer period structural behaviours have been revealed by total station measurements. The magnitudes of the displacements evaluated were compared with 95% confidence ellipses to determine the level of significance. The results showed that the tower moved approximately 3 cm during the monitoring period. The comparison of both methods in terms of accuracy was made using standard errors and showed that the GNSS method gave better results. However, RTS observations made from a distance of about 570 m were compatible with GNSS in detecting semi-static movements, showing that it has a significant measurement capacity. With this measuring capacity, it is clear that it will continue to maintain its place as an indispensable measuring device in many SHM studies.

This test study additionally indicates that RTS measurements taken over long distances can determine

static and quasi-static structure movements, and the results are verified using GNSS measurements. The results produced using both techniques were consistent and satisfactory. The determination of high-frequency structural movements using RTS is dependent on the devices having a less delayed reading and a higher frequency measurement capability during measurements. Automatic measurements from long distances with the electronic total station have been proven in SHM studies, and it is an alternative to GNSS.

References

Allan, A.L. (1988), "The principles of theodolite intersection systems", *Survey Review*, **29**(227), 226-234. https://doi.org/10.1179/sre.1988.29.227.226

Alsadik, B. (2019), "Chapter 4 - Observation Models and Least Squares Adjustment", In: *Adjustment Models in 3D Geomatics and Computational Geophysics*, pp. 89-151. https://doi.org/10.1016/b978-0-12-817588-0.00004-0

Breuer, P., Chmielewski, T., Górski, P., Konopka, E. and Tarczyński, L. (2015), "Monitoring horizontal displacements in a vertical profile of a tall industrial chimney using Global Positioning System technology for detecting dynamic characteristics", *Struct. Control Health Monitor.*, **22**(7), 1002-1023. https://doi.org/10.1002/stc.1730

Breuer, P., Chmielewski, T. and Górski, P. (2021), "Dynamic response of the Stuttgart TV tower measured by classical instruments and GPS technology", *Arch. Civil Eng.*, **67**(1). https://doi.org/10.24425/ace.2021.136459

Casciati, S. and Vece, M. (2017), "Real-time monitoring system for local storage and data transmission by remote control", *Adv. Eng. Software*, **112**, 46-53. https://doi.org/10.1016/j.advengsoft.2017.06.010

Chan, W.-S., Xu, Y.-L., Ding, X.-L., Xiong, Y.-L. and Dai, W.-J. (2006), "Assessment of dynamic measurement accuracy of GPS in three directions", *J. Survey. Eng.*, **132**(3), 108-117. https://doi.org/10.1061/(ASCE)0733-9453(2006)132:3(108)

Chatzi, E.N. and Fuggini, C. (2012), "Structural identification of a super-tall tower by GPS and accelerometer data fusion using a multi-rate Kalman filter", In: *Life-Cycle and Sustainability of Civil Infrastructure Systems*, *Proceedings of the 3rd International Symposium on Life-Cycle Civil Engineering*, *IALCCE 2012*, Vienna, Austria, October.

Cook, D. (2006), "Robotic total stations and remote data capture: Challenges in construct", In: *Geotechnical News* (Vol. 24, Issue 4).

Cosser, E., Roberts, G.W., Meng, X. and Dodson, A.H. (2003), "Measuring the dynamic deformation of bridges using a total station", *Proceedings of 11th FIG Symposium on Deformation Monitoring*, Santorini, Greece, May.

Ehigiator, M.O. and Ehigiator–Irughe, R. (2018), "Formulation and implementation of mathematical models suitable for deformation analysis of structures", *Nigerian J. Technol.*, **37**(2), 294-301. https://doi.org/10.4314/njt.v37i2.2

Ehigiator, M.O., Oladosu, S.O. and Ehigiator-Irughe, R. (2017), "Application of Least Squares Estimation Techniques in 2D Conformal Coordinates Transformation from Local to National", *Nigerian J. Environ. Sci. Technol.*, **1**(2), 71-84. https://doi.org/10.36263/nijest.2017.02.0039

Ehigiator-Irughe, R., Ehiorobo, J.O. and Ehigiator, M.O. (2010), "Distortion of oil and Gas infrastructure from Geomatics support view", *J. Emerg. Trends Eng. Appl. Sci.* (*JETEAS*), **1**, 14-23. https://hdl.handle.net/10520/EJC156745

Erdoğan, H. and Gülal, E. (2013), "Ambient vibration measurements of the Bosphorus suspension bridge by total station and GPS", *Experim. Techniq.*, **37**(3), 16-23. https://doi.org/10.1111/j.1747-1567.2011.00723.x

Frukacz, M., Presl, R., Wieser, A. and Favot, D. (2017), "Pushing the sensitivity limits of RTS-based continuous deformation monitoring of an alpine valley", *Appl. Geomat.*, **9**(2), 81-92. https://doi.org/10.1007/s12518-017-0182-2

Hatoum, H.M. and Mustafin, M.G. (2020), "Optimization of locating robotic total stations for determining the deformations of buildings and structures", *Geodezia i Kartografia*, **963**(9). https://doi.org/10.22389/0016-7126-2020-963-9-2-13

Jo, H., Sim, S.H., Tatkowski, A., Spencer, B.F. and Nelson, M.E. (2013), "Feasibility of displacement monitoring using low-cost GPS receivers", *Struct. Control Health Monitor.*, **20**(9), 1240-1254. https://doi.org/10.1002/stc.1532

Kaloop, M.R. and Li, H. (2009), "Tower bridge movement analysis with GPS and accelerometer techniques: Case study Yonghe tower bridge", *Inform. Technol. J.*, **8**(8), 1213-1220.

Kaloop, M.R., Elbeltagi, E. and Elnabwy, M.T. (2015), "Bridge monitoring with wavelet principal component and spectrum analysis based on GPS measurements: Case study of the Mansoura Bridge in Egypt", *J. Perform. Constr. Facil.*, **29**(3), p. 04014071. https://doi.org/10.1061/(ASCE)CF.1943-5509.0000559

Kaloop, M.R., Hu, J.W. and Elbeltagi, E. (2016), "Adjustment and assessment of the measurements of low and high sampling frequencies of GPS real-time monitoring of structural movement", *ISPRS Int. J. Geo-Inform.*, **5**(12), 222. https://doi.org/10.3390/ijgi5120222

Kovačič, B. and Motoh, T. (2019), "Determination of static and dynamic response of structures with geodetic methods in loading tests", *Acta Geodaetica et Geophysica*, **54**(2), 243-261. https://doi.org/10.1007/s40328-019-00251-x

Lekidis, V., Tsakiri, M., Makra, K., Karakostas, C., Klimis, N. and Sous, I. (2005), "Evaluation of dynamic response and local soil effects of the Evripos cable-stayed bridge using multi-sensor monitoring systems", *Eng. Geol.*, **79**(1-2), 43-59. https://doi.org/10.1016/j.enggeo.2004.10.015

Lienhart, W., Ehrhart, M. and Grick, M. (2017), "High frequent total station measurements for the monitoring of bridge vibrations", *J. Appl. Geodesy*, **11**(1), 1-8. https://doi.org/10.1515/jag-2016-0028

Meng, X., Dodson, A.H. and Roberts, G.W. (2007), "Detecting bridge dynamics with GPS and triaxial accelerometers", *Eng. Struct.*, **29**(11), 3178-3184. https://doi.org/10.1016/j.engstruct.2007.03.012

Moschas, F. and Stiros, S. (2011), "Measurement of the dynamic displacements and the modal frequencies of a short-span pedestrian bridge using GPS and an accelerometer", *Eng. Struct.*, **33**(1), 10-17. https://doi.org/10.1016/j.engstruct.2010.09.013

Moschas, F., Psimoulis, P.A. and Stiros, S.C. (2013), "GPS/RTS data fusion to overcome signal deficiencies in certain bridge dynamic monitoring projects", *Smart Struct. Syst., Int. J.*, **12**(3-4), 251-269. https://doi.org/10.12989/sss.2013.12.3_4.251

Okwuashi, O. and Asuquo, I. (2012), "Basics of Least Squares Adjustment Computation in Surveying", *Int. J. Sci. Res.* (*IJSR*), **3**(8), 188-193.

Park, H.S., Lee, H.M., Adeli, H. and Lee, I. (2007), "A new approach for health monitoring of structures: Terrestrial laser scanning", *Comput.-Aided Civil Infrastr. Eng.*, **22**(1), 19-30. https://doi.org/10.1111/j.1467-8667.2006.00466.x

Pehlivan, H. (2018), "Frequency analysis of GPS data for structural health monitoring observations", *Struct. Eng. Mech., Int. J.*, **66**(2), 185-193. https://doi.org/10.12989/sem.2018.66.2.185

Pehlivan, H. (2021), "The Analysis Methodology of Robotic Total

Station Data for Determination of Structural Displacements", *Adv. Geomat.*, **1**(1), 1-7.
Pehlivan, H. and Bayata, H.F. (2016), "Usability of inclinometers as a complementary measurement tool in structural monitoring", *Struct. Eng. Mech., Int. J.*, **58**(6), 1077-1085. https://doi.org/10.12989/sem.2016.58.6.1077
Pehlivan, H., Aydin, Ö., Gülal, E. and Bilgili, E. (2015), "Determining the behavior of high-rise structures with geodetic hybrid sensors", *Geomat. Nat. Hazards Risk*, **6**(8), 702-717. https://doi.org/10.1080/19475705.2013.854280
Psimoulis, P.A. and Stiros, S.C. (2007), "Measurement of deflections and of oscillation frequencies of engineering structures using Robotic Theodolites (RTS)", *Eng. Struct.*, **29**(12), 3312-3324. https://doi.org/10.1016/j.engstruct.2007.09.006
Psimoulis, P.A. and Stiros, S.C. (2008), "Experimental assessment of the accuracy of GPS and RTS for the determination of the parameters of oscillation of major structures", *Comput.-Aided Civil Infrastr. Eng.*, **23**(5), 389-403. https://doi.org/10.1111/j.1467-8667.2008.00547
Psimoulis, P. and Stiros, S. (2011), "Robotic theodolites (RTS): Measuring structure excitation", *GIM Int.*, **25**(4), 29-33.
Psimoulis, P. and Stiros, S. (2013), "Measuring deflections of a short-span railway bridge using a Robotic Total Station (RTS)", *J. Bridge Eng.*, **18**(2), 182-185. http://dx.doi.org/10.1061/(ASCE)BE.1943-5592.0000334
Psimoulis, P., Pytharouli, S., Karambalis, D. and Stiros, S. (2008), "Potential of Global Positioning System (GPS) to measure frequencies of oscillations of engineering structures", *J. Sound Vib.*, **318**(3), 606-623. https://doi.org/10.1016/j.jsv.2008.04.036
Radovanovic, R.S. and Teskey, W.F. (2001), "Dynamic monitoring of deforming structures: GPS versus robotic tacheometry systems", *Proceeding of the10th FIG International Symposium on Deformation Measurements*, Orange, CA, USA, March.
Roberts, G.W., Meng, X. and Dodson, A.H. (2004), "Integrating a global positioning system and accelerometers to monitor the deflection of bridges", *J. Survey. Eng.*, **130**(2), 65-72. https://doi.org/10.1061/(ASCE)0733-9453(2004)130:2(65)
Shen, N., Chen, L., Liu, J., Wang, L., Tao, T., Wu, D. and Chen, R. (2019), "A review of global navigation satellite system (GNSS)-based dynamic monitoring technologies for structural health monitoring", *Remote Sensing*, **11**(9), p. 1001. https://doi.org/10.3390/rs11091001
Stiros, S., Psimoulis, P., Moschas, F., Saltogianni, V., Tsantopoulos, E. and Triantafyllidis, P. (2019), "Multi-sensor measurement of dynamic deflections and structural health monitoring of flexible and stiff bridges", *Bridge Struct.*, **15**(1-2), 43-51. https://doi.org/10.3233/BRS-190152
Trimble (2021), https://geospatial.trimble.com/products-and-solutions/trimble-s5.htm.
Wang, X., Zhao, Q., Xi, R., Li, C., Li, G. and Li, L. (2021), "Review of bridge structural health monitoring based on GNSS: from displacement monitoring to dynamic characteristic identification", *IEEE Access*, **9**, 80043-80065 https://doi.org/10.1109/ACCESS.2021.3083749
Xu, L., Guo, J.J. and Jiang, J.J. (2002), "Time-frequency analysis of a suspension bridge based on GPS", *J. Sound Vib.*, **254**(1), 105-116. https://doi.org/10.1006/jsvi.2001.4087
Yigit, C.O., Coskun, M.Z., Yavasoglu, H., Arslan, A. and Kalkan, Y. (2016), "The potential of GPS Precise Point Positioning method for point displacement monitoring: A case study", *Measurement*, **91**, 398-404. https://doi.org/10.1016/j.measurement.2016.05.074
Yu, J., Meng, X., Shao, X., Yan, B. and Yang, L. (2014), "Identification of dynamic displacements and modal frequencies of a medium-span suspension bridge using multimode GNSS processing", *Eng. Struct.*, **81**, 432-443. https://doi.org/10.1016/j.engstruct.2014.10.010
Yu, J., Yan, B., Meng, X., Shao, X. and Ye, H. (2016), "Measurement of bridge dynamic responses using network-based real-time kinematic GNSS technique", *J. Survey. Eng.*, **142**(3), p. 04015013.
Yu, J., Fang, Z., Meng, X., Xie, Y. and Fan, Q. (2020), "Measurement of quasi-static and dynamic displacements of footbridges using the composite instrument of a smartstation and an accelerometer: Case studies", *Remote Sensing*, **12**(16), 2635. https://doi.org/10.3390/RS12162635
Zhao, X., Liu, H., Yu, Y., Xu, X., Hu, W., Li, M. and Ou, J. (2015), "Bridge displacement monitoring method based on laser projection-sensing technology", *Sensors*, **15**(4), 8444-8463. https://doi.org/10.3390/s150408444
Zhou, J., Xiao, H., Jiang, W., Bai, W. and Liu, G. (2020), "Automatic subway tunnel displacement monitoring using robotic total station", *Measurement*, **151**, p. 107251. https://doi.org/10.1016/j.measurement.2019.107251
Zhou, J., Shi, B., Liu, G. and Ju, S. (2021), "Accuracy analysis of dam deformation monitoring and correction of refraction with robotic total station", *PLoS ONE*, **16**, p. e0251281. https://doi.org/10.1371/journal.pone.0251281

FC